

Supplemental Data

Insights into the Nature of DNA Binding

of AbrB-like Transcription Factors

Daniel M. Sullivan, Benjamin G. Bobay, Douglas J. Kojetin, Richele J. Thompson, Mark Rance, Mark A. Strauch, and John Cavanagh

```

AbrBN_BACSU      MKSTGIVRKVDELGRVVIPIELRRTLGLIAEKDALEIYVDDE-KIILKKYKPNMT-
AbhN_BACSU       MKSIGVVRKVDELGRIVMPIELRRALDIAIKDSIEFFVDGD-KIILKKYKPHGVC
SpoVTN_BACSU     MKATGIVRRIDDLGRVVIPKEIRRTLRIREGDPLEIFVDRDGEVILKKYSPISEL
** : *::*::*::*::*::*::* *::*::* *  *::*::*::* : ::*::*::*

```

Figure S1. Multiple Sequence Alignment of AbrBN, AbhN, and SpoVTN

N-terminal sequence alignment of AbrB, Abh, and SpoVT from *B. subtilis*. Identical residues are marked by an *asterisk*, strongly similar residues are marked by a *colon*, somewhat similar residues are marked by a *dot*, and dissimilar residues are not marked.

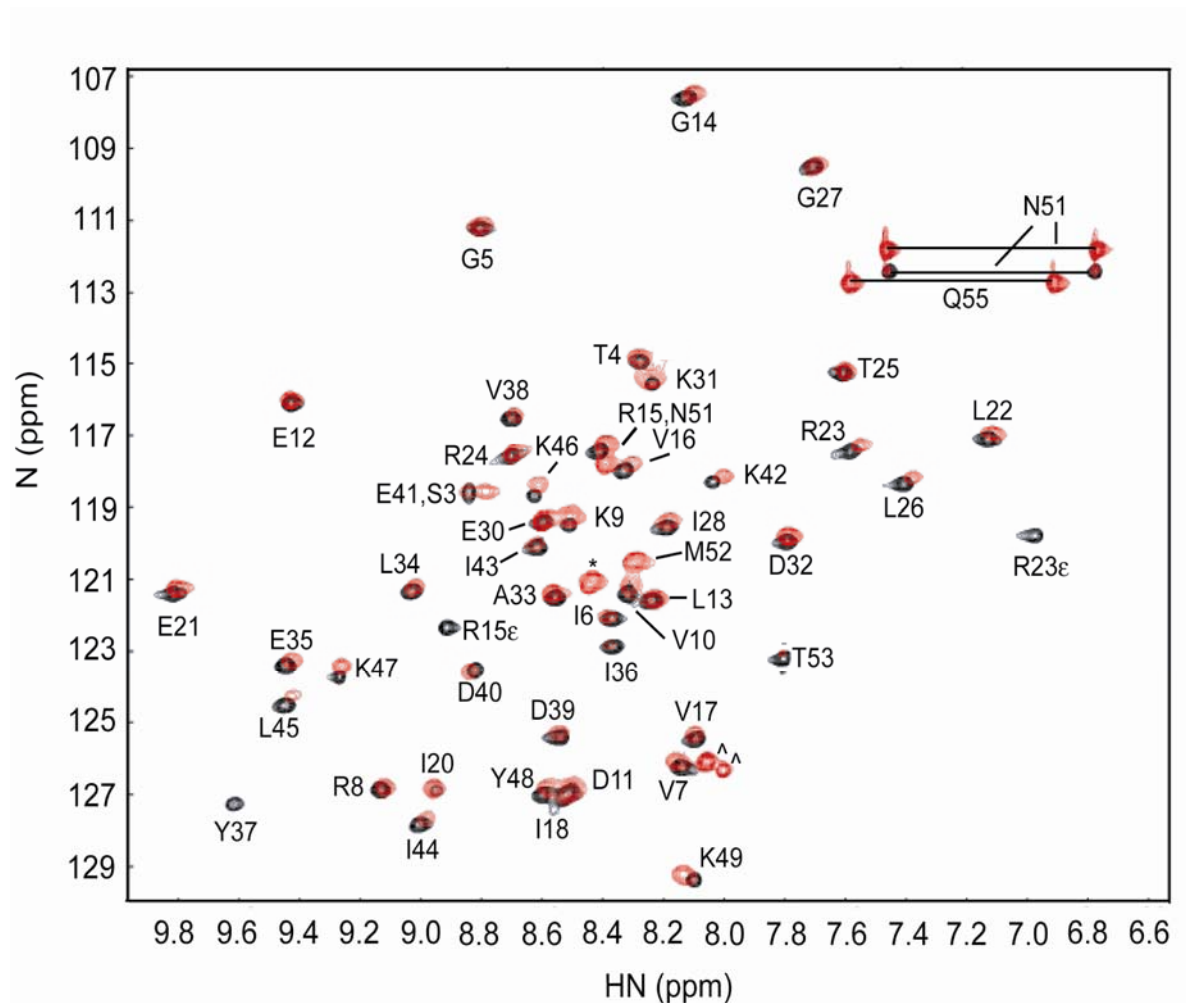


Figure S2. ^{15}N HSQC Spectra Overlay of AbrBN and AbrBN⁵⁵-Tetramer

AbrBN spectra denoted with black peaks while AbrBN⁵⁵-tetramer spectra denoted with red peaks. Spectrum is labeled with AbrBN assignments. Q55 is only present in AbrBN⁵⁵-tetramer as

it is the 55th residue. The ^ symbol denotes extra peaks in the AbrBN⁵⁵ spectra that can be attributed to residues C54 and Q55 while, the * symbol denotes a possible NH side chain. Results suggest that no major structural change takes place when AbrBN⁵⁵-tetramer is oxidized, suggesting a modeling strategy using oxidized AbrBN⁵⁵-tetramer as the binder is warranted.

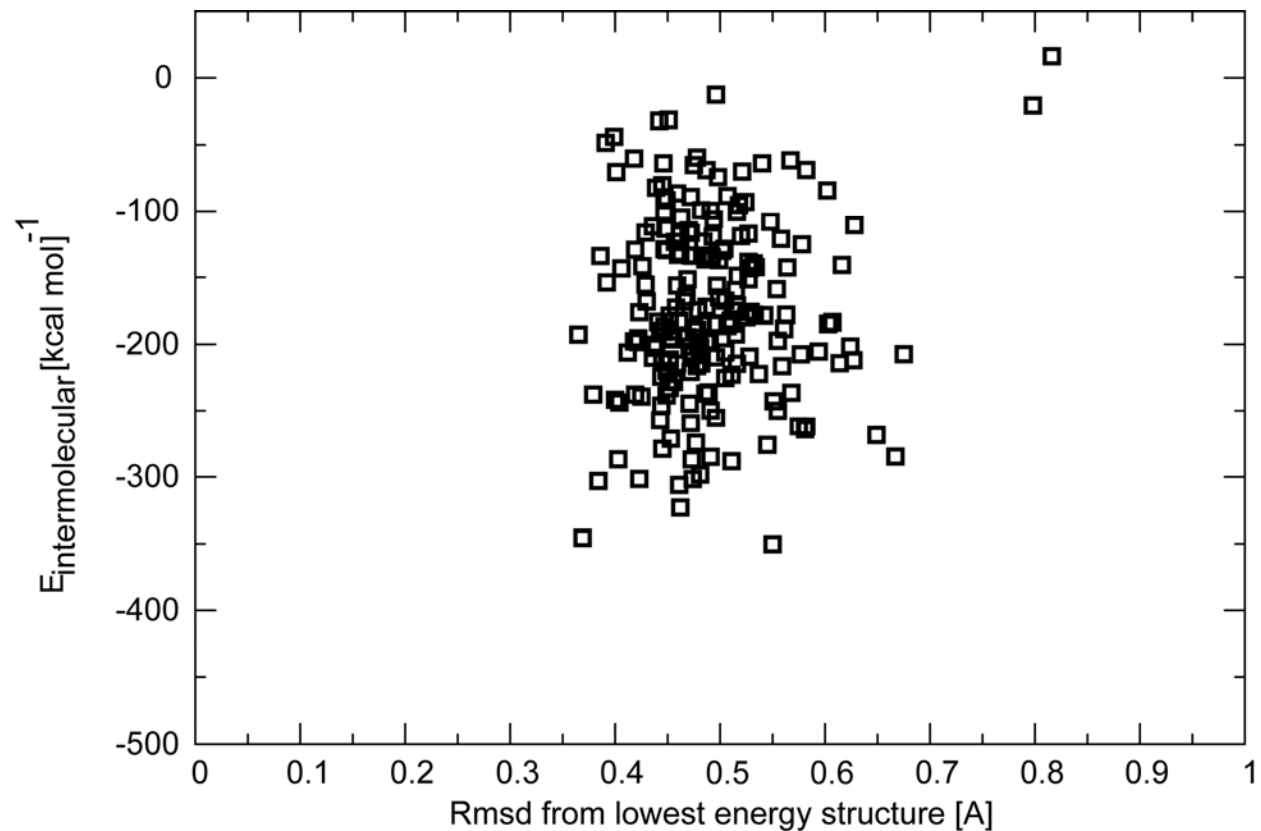


Figure S3. HADDOCK Score Versus RMSD for the AbrBN⁵⁵-Tetramer in Complex with *abrB8* (Semi-Flexible Docking Protocol)

The results show one cluster of structures with an r.m.s.d. range of 1.5 to 3.0Å for two hundred water refined complexes from the semi-flexible HADDOCK docking protocol. The E_{inter} is similar to published HADDOCK protein-DNA docking (van Dijk *et al.*, 2006). The solution in the semi-flexible docking appears to be very similar with respect to the protein and the spatial arrangement of the complex.

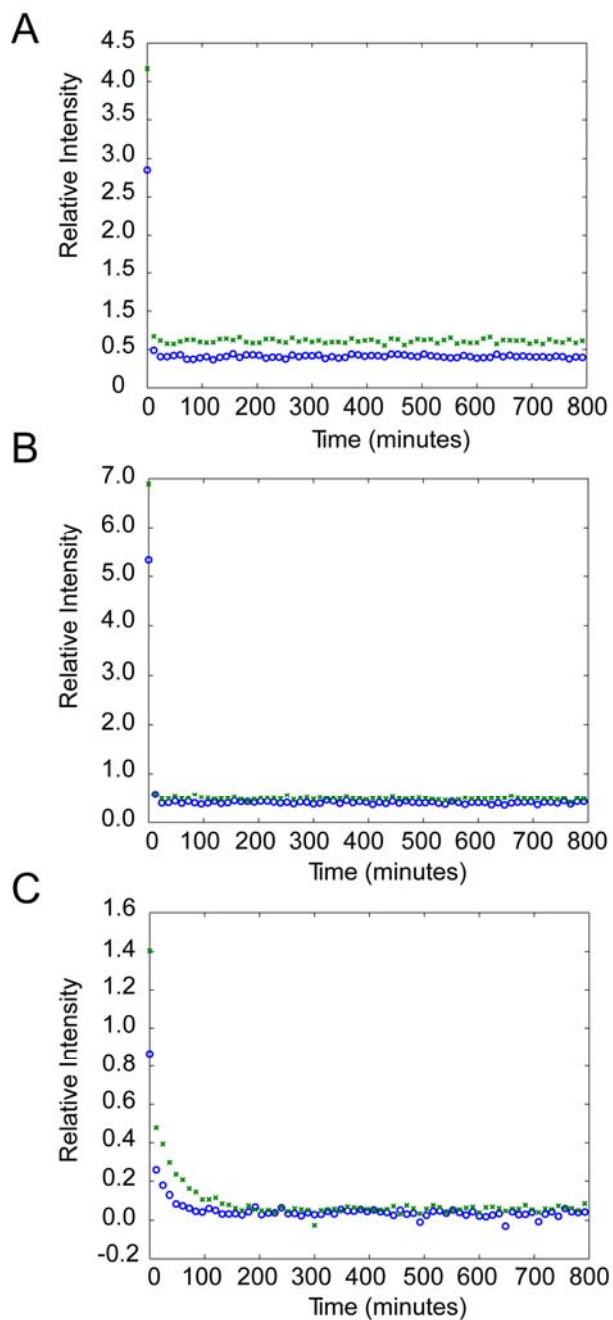


Figure S4. Hydrogen Exchange Data for the “GD-Box” Region of AbrBN, AbhN and SpoVTN

Sixty-six sequential twelve minute ^1H - ^{15}N HSQC were recorded to determine exchange protected amide protons.

(A) AbrBN

(B) AbhN

(C) SpoVTN.

“o” is residue 10 and “x” is residue 32.

Supplementary Table 1. AbhN ¹⁵N relaxation and dynamics parameters (pH 5.8, 305.15 K, 399.8636182 MHz)

Residue	R_1 (s^{-1})	R_2 (s^{-1})	NOE	Model	S^2	S_f^2	$\tau_e < 100$ or τ_f (ps)	$\tau_e > 100$ or τ_s (ps)	R_{ex} (s^{-1})
<i>Monomer A</i>									
M1									
K2									
S3	2.15 ± 0.04	5.66 ± 0.10	0.22 ± 0.01	m2	0.574 ± 0.007			120 ± 5	
I4	2.35 ± 0.05	7.87 ± 0.15	0.32 ± 0.02	m4	0.646 ± 0.013			126 ± 11	1.57 ± 0.20
G5	2.54 ± 0.08	10.93 ± 0.30	0.43 ± 0.04	m4	0.718 ± 0.024			129 ± 23	3.99 ± 0.37
V6									
V7	2.71 ± 0.05	7.07 ± 0.13	0.68 ± 0.02	m5	0.689 ± 0.038	0.820 ± 0.015		3497 ± 1593	
R8	2.86 ± 0.04	7.42 ± 0.11	0.67 ± 0.02	m5	0.719 ± 0.031	0.869 ± 0.011		3311 ± 963	
K9	2.64 ± 0.06	8.82 ± 0.19	0.64 ± 0.03	m4	0.785 ± 0.017		55 ± 15		1.37 ± 0.22
V10	2.68 ± 0.04	8.12 ± 0.10	0.67 ± 0.02	m4	0.801 ± 0.011		44 ± 9		0.54 ± 0.16
D11	2.74 ± 0.05	10.99 ± 0.18	0.71 ± 0.02	m4	0.827 ± 0.014		26 ± 14		3.20 ± 0.23
E12	2.70 ± 0.03	8.40 ± 0.09	0.63 ± 0.01	m4	0.800 ± 0.009		67 ± 8		0.81 ± 0.12
L13	2.82 ± 0.04	8.63 ± 0.11	0.67 ± 0.02	m4	0.843 ± 0.011		59 ± 12		0.66 ± 0.16
G14	2.76 ± 0.04	8.40 ± 0.11	0.71 ± 0.02	m4	0.831 ± 0.012		27 ± 11		0.55 ± 0.15
R15									
I16	2.71 ± 0.04	9.01 ± 0.13	0.69 ± 0.02	m4	0.814 ± 0.013		35 ± 13		1.32 ± 0.17
V17	2.62 ± 0.04	8.03 ± 0.10	0.68 ± 0.02	m4	0.786 ± 0.012		34 ± 8		0.60 ± 0.13
M18	2.70 ± 0.04	7.75 ± 0.10	0.67 ± 0.02	m2	0.814 ± 0.008		44 ± 9		
P19									
I20	2.76 ± 0.05	8.07 ± 0.12	0.64 ± 0.02	m4	0.820 ± 0.015		70 ± 12		0.29 ± 0.18
E21	2.70 ± 0.03	7.99 ± 0.09	0.70 ± 0.01	m4	0.812 ± 0.009		28 ± 7		0.33 ± 0.12
L22	2.81 ± 0.04	7.54 ± 0.10	0.64 ± 0.02	m5	0.763 ± 0.021	0.871 ± 0.013		1921 ± 554	
R23	2.70 ± 0.03	7.51 ± 0.10	0.65 ± 0.01	m2	0.798 ± 0.007		55 ± 9		
R24	2.71 ± 0.03	7.70 ± 0.09	0.66 ± 0.01	m2	0.810 ± 0.006		53 ± 7		
A25	2.70 ± 0.03	7.75 ± 0.08	0.70 ± 0.01	m2	0.817 ± 0.005		26 ± 7		
L26	2.74 ± 0.04	7.82 ± 0.10	0.68 ± 0.02	m2	0.825 ± 0.008		40 ± 12		
D27									
I28	2.68 ± 0.04	8.30 ± 0.11	0.71 ± 0.02	m4	0.809 ± 0.013		21 ± 10		0.67 ± 0.16
A29	2.64 ± 0.04	8.14 ± 0.11	0.66 ± 0.02	m4	0.788 ± 0.012		46 ± 10		0.68 ± 0.15
I30	2.71 ± 0.03	7.22 ± 0.08	0.66 ± 0.01	m5	0.725 ± 0.020	0.833 ± 0.008		2396 ± 563	
K31	2.77 ± 0.05	8.79 ± 0.15	0.68 ± 0.03	m4	0.830 ± 0.017		48 ± 19		0.93 ± 0.22
D32	2.74 ± 0.03	7.87 ± 0.09	0.69 ± 0.01	m2	0.828 ± 0.007		38 ± 8		
S33	2.53 ± 0.03	6.73 ± 0.09	0.66 ± 0.02	m5	0.673 ± 0.023	0.777 ± 0.010		2587 ± 766	
I34	2.87 ± 0.07	9.47 ± 0.19	0.66 ± 0.03	m4	0.855 ± 0.021		69 ± 28		1.37 ± 0.29
E35	2.93 ± 0.04	8.12 ± 0.11	0.69 ± 0.02	m2	0.869 ± 0.009		57 ± 18		
F36	2.82 ± 0.05	7.80 ± 0.13	0.69 ± 0.02	m2	0.834 ± 0.011		43 ± 16		
F37	2.79 ± 0.04	7.38 ± 0.11	0.68 ± 0.02	m5	0.732 ± 0.029	0.849 ± 0.015		3043 ± 1162	
V38	2.59 ± 0.04	9.34 ± 0.11	0.67 ± 0.02	m4	0.775 ± 0.011		37 ± 9		2.00 ± 0.15
D39	2.73 ± 0.04	7.66 ± 0.10	0.68 ± 0.02	m2	0.815 ± 0.008		38 ± 10		

Supplementary Table 1 continued

Supplementary Table 1. AbhN ¹⁵N relaxation and dynamics parameters (pH 5.8, 305.15 K, 399.8636182 MHz)

Residue	R_1 (s^{-1})	R_2 (s^{-1})	NOE	Model	S^2	S_f^2	$\tau_e < 100$ or τ_f (ps)	$\tau_e > 100$ or τ_s (ps)	R_{ex} (s^{-1})
A25	2.70 ± 0.03	7.75 ± 0.08	0.70 ± 0.01	m2	0.817 ± 0.006		26 ± 7		
L26	2.74 ± 0.04	7.82 ± 0.10	0.68 ± 0.02	m2	0.825 ± 0.008		40 ± 12		
D27									
I28	2.68 ± 0.04	8.30 ± 0.11	0.71 ± 0.02	m4	0.809 ± 0.013		21 ± 10		0.67 ± 0.16
A29	2.64 ± 0.04	8.14 ± 0.11	0.66 ± 0.02	m4	0.788 ± 0.012		46 ± 10		0.68 ± 0.15
I30	2.71 ± 0.03	7.22 ± 0.08	0.66 ± 0.01	m5	0.725 ± 0.019	0.833 ± 0.009		2396 ± 537	
K31	2.77 ± 0.05	8.79 ± 0.15	0.68 ± 0.03	m4	0.830 ± 0.017		48 ± 19		0.93 ± 0.21
D32	2.74 ± 0.03	7.87 ± 0.09	0.69 ± 0.01	m2	0.828 ± 0.007		38 ± 8		
S33	2.53 ± 0.03	6.73 ± 0.09	0.66 ± 0.02	m5	0.673 ± 0.024	0.777 ± 0.021		2587 ± 844	
I34	2.87 ± 0.07	9.47 ± 0.19	0.66 ± 0.03	m4	0.855 ± 0.020		69 ± 27		1.37 ± 0.27
E35	2.93 ± 0.04	8.12 ± 0.11	0.69 ± 0.02	m2	0.869 ± 0.008		57 ± 17		
F36	2.82 ± 0.05	7.80 ± 0.13	0.69 ± 0.02	m2	0.834 ± 0.010		43 ± 16		
F37	2.79 ± 0.04	7.38 ± 0.11	0.68 ± 0.02	m5	0.732 ± 0.031	0.849 ± 0.012		3043 ± 1264	
V38	2.59 ± 0.04	9.34 ± 0.11	0.67 ± 0.02	m4	0.775 ± 0.010		37 ± 8		2.00 ± 0.14
D39	2.73 ± 0.04	7.66 ± 0.10	0.68 ± 0.02	m2	0.815 ± 0.007		38 ± 10		
G40	2.56 ± 0.05	6.95 ± 0.12	0.68 ± 0.02	m5	0.709 ± 0.029	0.787 ± 0.049		2261 ± 1195	
D41	2.52 ± 0.03	6.31 ± 0.08	0.64 ± 0.01	m5	0.590 ± 0.024	0.766 ± 0.009		3216 ± 546	
K42	2.66 ± 0.04	7.86 ± 0.10	0.64 ± 0.02	m4	0.787 ± 0.012		58 ± 9		0.39 ± 0.16
I43	2.78 ± 0.04	8.69 ± 0.12	0.66 ± 0.02	m4	0.827 ± 0.013		60 ± 14		0.85 ± 0.17
I44	2.84 ± 0.04	9.09 ± 0.13	0.69 ± 0.02	m4	0.852 ± 0.014		47 ± 18		1.04 ± 0.18
L45	2.86 ± 0.05	7.77 ± 0.13	0.71 ± 0.03	m5	0.787 ± 0.033	0.865 ± 0.027		3938 ± 2066	
K46									
K47	2.75 ± 0.04	7.21 ± 0.10	0.61 ± 0.02	m5	0.715 ± 0.023	0.860 ± 0.011		1922 ± 402	
Y48	2.86 ± 0.04	7.37 ± 0.10	0.65 ± 0.02	m5	0.711 ± 0.026	0.871 ± 0.010		3031 ± 716	
K49									
P50									
H51									
G52	1.40 ± 0.04	2.59 ± 0.11	-0.77 ± 0.02	m5	0.185 ± 0.022	0.607 ± 0.020		732 ± 108	
V53	1.16 ± 0.02	1.55 ± 0.05	-1.38 ± 0.01	m5	0.051 ± 0.010	0.558 ± 0.007		808 ± 33	
C54	0.83 ± 0.01	1.03 ± 0.04	-1.79 ± 0.01	m5	0.025 ± 0.008	0.434 ± 0.006		692 ± 35	

Supplementary Table 2 continued

Supplementary Table 2. AbrBN ^{15}N relaxation and dynamics parameters (pH 5.8, 305.15 K, 399.8636182 MHz)

Residue	R_1 (s^{-1})	R_2 (s^{-1})	NOE	Model	S^2	S_f^2	$\tau_e < 100$ or τ_f (ps)	$\tau_e > 100$ or τ_s (ps)	R_{ex} (s^{-1})
<i>Monomer A</i>									
M1									
K2									
S3	2.17 ± 0.06	5.56 ± 0.18	0.29 ± 0.03	<i>m2</i>	0.582 ± 0.013			103 ± 9	
T4	2.35 ± 0.03	5.29 ± 0.12	0.42 ± 0.02	<i>m5</i>	0.442 ± 0.025	0.759 ± 0.010		2060 ± 177	
G5	2.50 ± 0.03	5.75 ± 0.11	0.50 ± 0.01	<i>m5</i>	0.484 ± 0.026	0.786 ± 0.009		2496 ± 227	
I6	2.69 ± 0.03	8.09 ± 0.12	0.72 ± 0.01	<i>m2</i>	0.829 ± 0.007		20 ± 8		
V7	2.67 ± 0.03	7.45 ± 0.12	0.66 ± 0.02	<i>m2</i>	0.793 ± 0.008		42 ± 10		
R8	2.77 ± 0.04	7.44 ± 0.13	0.67 ± 0.02	<i>m2</i>	0.812 ± 0.008		43 ± 11		
K9	2.56 ± 0.04	7.17 ± 0.15	0.61 ± 0.02	<i>m2</i>	0.755 ± 0.009		56 ± 11		
V10	2.60 ± 0.03	7.71 ± 0.13	0.69 ± 0.02	<i>m2</i>	0.793 ± 0.008		33 ± 9		
D11									
E12	2.66 ± 0.03	7.11 ± 0.11	0.68 ± 0.01	<i>m5</i>	0.675 ± 0.031	0.811 ± 0.009		3694 ± 1049	
L13	2.81 ± 0.03	7.80 ± 0.12	0.72 ± 0.02	<i>m2</i>	0.841 ± 0.008		23 ± 11		
G14	2.73 ± 0.04	7.99 ± 0.12	0.69 ± 0.02	<i>m4</i>	0.811 ± 0.011		30 ± 9		0.46 ± 0.17
R15	2.84 ± 0.04	7.88 ± 0.13	0.70 ± 0.02	<i>m2</i>	0.848 ± 0.008		32 ± 12		
V16	2.73 ± 0.04	8.95 ± 0.17	0.77 ± 0.02	<i>m3</i>	0.836 ± 0.012				0.98 ± 0.21
V17	2.61 ± 0.03	8.35 ± 0.14	0.67 ± 0.02	<i>m4</i>	0.797 ± 0.010		41 ± 10		0.57 ± 0.17
I18									
P19									
I20	2.69 ± 0.05	7.95 ± 0.18	0.71 ± 0.02	<i>m2</i>	0.823 ± 0.011		28 ± 14		
E21	2.78 ± 0.04	7.94 ± 0.13	0.68 ± 0.02	<i>m5</i>	0.787 ± 0.027	0.872 ± 0.021		2044 ± 892	
L22	2.77 ± 0.03	7.70 ± 0.13	0.68 ± 0.02	<i>m2</i>	0.824 ± 0.009		48 ± 13		
R23	2.66 ± 0.04	7.72 ± 0.14	0.66 ± 0.02	<i>m2</i>	0.802 ± 0.009		48 ± 10		
R24	2.69 ± 0.03	8.08 ± 0.13	0.69 ± 0.01	<i>m2</i>	0.826 ± 0.007		39 ± 9		
T25	2.59 ± 0.03	7.60 ± 0.11	0.68 ± 0.01	<i>m2</i>	0.787 ± 0.007		33 ± 7		
L26	2.72 ± 0.03	7.76 ± 0.13	0.69 ± 0.02	<i>m2</i>	0.819 ± 0.009		40 ± 12		
G27	2.66 ± 0.03	7.58 ± 0.12	0.70 ± 0.02	<i>m2</i>	0.801 ± 0.008		28 ± 9		
I28	2.58 ± 0.03	7.87 ± 0.13	0.68 ± 0.02	<i>m4</i>	0.782 ± 0.010		31 ± 8		0.37 ± 0.15
A29	2.60 ± 0.03	7.20 ± 0.12	0.65 ± 0.02	<i>m2</i>	0.768 ± 0.008		46 ± 7		
E30	2.59 ± 0.03	6.61 ± 0.10	0.59 ± 0.01	<i>m5</i>	0.606 ± 0.021	0.810 ± 0.007		2482 ± 278	
K31	2.61 ± 0.04	7.11 ± 0.14	0.57 ± 0.02	<i>m2</i>	0.756 ± 0.009		79 ± 11		
D32	2.72 ± 0.03	7.53 ± 0.10	0.66 ± 0.01	<i>m5</i>	0.762 ± 0.020	0.848 ± 0.018		1809 ± 531	
A33	2.36 ± 0.02	6.88 ± 0.10	0.55 ± 0.01	<i>m4</i>	0.688 ± 0.007		62 ± 4		0.25 ± 0.12
L34	2.62 ± 0.03	7.28 ± 0.14	0.67 ± 0.02	<i>m2</i>	0.778 ± 0.008		37 ± 9		
E35	2.79 ± 0.04	7.80 ± 0.14	0.68 ± 0.02	<i>m2</i>	0.832 ± 0.009		43 ± 14		
I36	2.81 ± 0.04	8.11 ± 0.17	0.71 ± 0.03	<i>m1</i>	0.856 ± 0.010				
Y37	2.89 ± 0.06	12.00 ± 0.29	0.70 ± 0.04	<i>m3</i>	0.873 ± 0.018				3.88 ± 0.33
V38	2.68 ± 0.04	8.04 ± 0.14	0.71 ± 0.02	<i>m4</i>	0.812 ± 0.011		21 ± 12		0.36 ± 0.17
D39	2.75 ± 0.03	7.83 ± 0.13	0.68 ± 0.02	<i>m2</i>	0.825 ± 0.008		39 ± 11		

Supplementary Table 2 continued

Supplementary Table 2. AbrBN ¹⁵N relaxation and dynamics parameters (pH 5.8, 305.15 K, 399.8636182 MHz)

Residue	R_1 (s^{-1})	R_2 (s^{-1})	NOE	Model	S^2	S_f^2	$\tau_e < 100$ or τ_f (ps)	$\tau_e > 100$ or τ_s (ps)	R_{ex} (s^{-1})
D40	2.51 ± 0.05	8.41 ± 0.18	0.68 ± 0.02	<i>m4</i>	0.758 ± 0.015		31 ± 9		1.13 ± 0.23
E41	2.55 ± 0.05	17.06 ± 0.40	0.61 ± 0.03	<i>m4</i>	0.744 ± 0.016		55 ± 12		10.10 ± 0.40
K42	2.67 ± 0.04	8.11 ± 0.16	0.62 ± 0.03	<i>m4</i>	0.785 ± 0.013		67 ± 15		0.70 ± 0.20
I43	2.75 ± 0.04	8.04 ± 0.15	0.68 ± 0.02	<i>m2</i>	0.833 ± 0.010		41 ± 15		
I44	2.81 ± 0.04	7.91 ± 0.15	0.70 ± 0.02	<i>m2</i>	0.843 ± 0.010		34 ± 17		
L45	2.77 ± 0.04	8.29 ± 0.16	0.70 ± 0.02	<i>m4</i>	0.835 ± 0.013		31 ± 17		0.40 ± 0.20
K46	2.74 ± 0.05	7.93 ± 0.17	0.66 ± 0.03	<i>m2</i>	0.826 ± 0.012		51 ± 20		
K47	2.65 ± 0.04	7.37 ± 0.14	0.67 ± 0.02	<i>m2</i>	0.787 ± 0.010		40 ± 12		
Y48	2.72 ± 0.03	7.51 ± 0.12	0.65 ± 0.02	<i>m2</i>	0.803 ± 0.008		55 ± 10		
K49	2.36 ± 0.03	5.84 ± 0.12	0.38 ± 0.02	<i>m5</i>	0.576 ± 0.025	0.781 ± 0.023		1066 ± 246	
P50									
N51	1.75 ± 0.03	3.62 ± 0.10	-0.25 ± 0.02	<i>m5</i>	0.286 ± 0.019	0.677 ± 0.010		947 ± 82	
M52	1.30 ± 0.02	2.14 ± 0.08	-2.18 ± 0.05	<i>m2</i>	0.123 ± 0.005			225 ± 7	
T53	0.79 ± 0.01	0.99 ± 0.07	-2.31 ± 0.01	<i>m5</i>	0.027 ± 0.012	0.466 ± 0.015		493 ± 61	
<i>Monomer B</i>									
M1									
K2									
S3	2.17 ± 0.06	5.56 ± 0.18	0.29 ± 0.03	<i>m2</i>	0.582 ± 0.014			102 ± 9	
T4	2.35 ± 0.03	5.29 ± 0.12	0.42 ± 0.02	<i>m5</i>	0.440 ± 0.025	0.759 ± 0.011		2068 ± 175	
G5	2.50 ± 0.03	5.75 ± 0.11	0.50 ± 0.01	<i>m5</i>	0.479 ± 0.026	0.786 ± 0.009		2528 ± 222	
I6	2.69 ± 0.03	8.09 ± 0.12	0.72 ± 0.01	<i>m2</i>	0.828 ± 0.007		20 ± 8		
V7	2.67 ± 0.03	7.45 ± 0.12	0.66 ± 0.02	<i>m2</i>	0.793 ± 0.008		45 ± 9		
R8	2.77 ± 0.04	7.44 ± 0.13	0.67 ± 0.02	<i>m2</i>	0.812 ± 0.009		43 ± 11		
K9	2.56 ± 0.04	7.17 ± 0.15	0.61 ± 0.02	<i>m2</i>	0.755 ± 0.010		57 ± 11		
V10	2.60 ± 0.03	7.71 ± 0.13	0.69 ± 0.02	<i>m2</i>	0.793 ± 0.008		33 ± 9		
D11									
E12	2.66 ± 0.03	7.11 ± 0.11	0.68 ± 0.01	<i>m5</i>	0.715 ± 0.026	0.811 ± 0.018		2835 ± 945	
L13	2.81 ± 0.03	7.80 ± 0.12	0.72 ± 0.02	<i>m5</i>	0.783 ± 0.029	0.856 ± 0.018		4082 ± 1778	
G14	2.73 ± 0.04	7.99 ± 0.12	0.69 ± 0.02	<i>m4</i>	0.811 ± 0.011		30 ± 10		0.46 ± 0.15
R15	2.84 ± 0.04	7.88 ± 0.13	0.70 ± 0.02	<i>m2</i>	0.848 ± 0.009		32 ± 12		
V16	2.73 ± 0.04	8.95 ± 0.17	0.77 ± 0.02	<i>m3</i>	0.832 ± 0.012				1.09 ± 0.20
V17	2.61 ± 0.03	8.35 ± 0.14	0.67 ± 0.02	<i>m4</i>	0.796 ± 0.010		41 ± 9		0.58 ± 0.18
I18									
P19									
I20	2.69 ± 0.05	7.95 ± 0.18	0.71 ± 0.02	<i>m2</i>	0.824 ± 0.013		27 ± 14		
E21	2.78 ± 0.04	7.94 ± 0.13	0.68 ± 0.02	<i>m5</i>	0.790 ± 0.025	0.872 ± 0.021		1985 ± 892	
L22	2.77 ± 0.03	7.70 ± 0.13	0.68 ± 0.02	<i>m2</i>	0.824 ± 0.009		46 ± 12		
R23	2.66 ± 0.04	7.72 ± 0.14	0.66 ± 0.02	<i>m2</i>	0.802 ± 0.009		47 ± 11		
R24	2.69 ± 0.03	8.08 ± 0.13	0.69 ± 0.01	<i>m2</i>	0.825 ± 0.008		39 ± 10		
T25	2.59 ± 0.03	7.60 ± 0.11	0.68 ± 0.01	<i>m2</i>	0.787 ± 0.007		34 ± 7		

Supplementary Table 2 continued

Supplementary Table 2. AbrBN ^{15}N relaxation and dynamics parameters (pH 5.8, 305.15 K, 399.8636182 MHz)

Residue	R_1 (s^{-1})	R_2 (s^{-1})	NOE	Model	S^2	S_f^2	$\tau_e < 100$ or τ_f (ps)	$\tau_e > 100$ or τ_s (ps)	R_{ex} (s^{-1})
L26	2.72 ± 0.03	7.76 ± 0.13	0.69 ± 0.02	m2	0.819 ± 0.009		39 ± 11		
G27	2.66 ± 0.03	7.58 ± 0.12	0.70 ± 0.02	m2	0.801 ± 0.008		28 ± 8		
I28	2.58 ± 0.03	7.87 ± 0.13	0.68 ± 0.02	m4	0.785 ± 0.010		32 ± 8		0.29 ± 0.15
A29	2.60 ± 0.03	7.20 ± 0.12	0.65 ± 0.02	m2	0.768 ± 0.008		46 ± 7		
E30	2.59 ± 0.03	6.61 ± 0.10	0.59 ± 0.01	m5	0.604 ± 0.021	0.810 ± 0.007		2500 ± 253	
K31	2.61 ± 0.04	7.11 ± 0.14	0.57 ± 0.02	m2	0.756 ± 0.010		79 ± 12		
D32	2.72 ± 0.03	7.53 ± 0.10	0.66 ± 0.01	m5	0.769 ± 0.021	0.847 ± 0.033		1635 ± 608	
A33	2.36 ± 0.02	6.88 ± 0.10	0.55 ± 0.01	m4	0.687 ± 0.007		61 ± 4		0.28 ± 0.12
L34	2.62 ± 0.03	7.28 ± 0.14	0.67 ± 0.02	m2	0.778 ± 0.008		36 ± 9		
E35	2.79 ± 0.04	7.80 ± 0.14	0.68 ± 0.02	m2	0.832 ± 0.009		43 ± 14		
I36	2.81 ± 0.04	8.11 ± 0.17	0.71 ± 0.03	m1	0.856 ± 0.011				
Y37	2.89 ± 0.06	12.00 ± 0.29	0.70 ± 0.04	m3	0.873 ± 0.018				3.88 ± 0.35
V38	2.68 ± 0.04	8.04 ± 0.14	0.71 ± 0.02	m4	0.810 ± 0.012		20 ± 11		0.41 ± 0.17
D39	2.75 ± 0.03	7.83 ± 0.13	0.68 ± 0.02	m2	0.825 ± 0.009		38 ± 11		
D40	2.51 ± 0.05	8.41 ± 0.18	0.68 ± 0.02	m4	0.756 ± 0.015		31 ± 9		1.18 ± 0.21
E41	2.55 ± 0.05	17.06 ± 0.40	0.61 ± 0.03	m4	0.744 ± 0.015		55 ± 11		10.11 ± 0.44
K42	2.67 ± 0.04	8.11 ± 0.16	0.62 ± 0.03	m4	0.783 ± 0.013		67 ± 15		0.73 ± 0.19
I43	2.75 ± 0.04	8.04 ± 0.15	0.68 ± 0.02	m4	0.823 ± 0.011		40 ± 14		0.28 ± 0.17
I44	2.81 ± 0.04	7.91 ± 0.15	0.70 ± 0.02	m2	0.843 ± 0.011		34 ± 17		
L45	2.77 ± 0.04	8.29 ± 0.16	0.70 ± 0.02	m4	0.835 ± 0.014		31 ± 16		0.40 ± 0.19
K46	2.74 ± 0.05	7.93 ± 0.17	0.66 ± 0.03	m4	0.812 ± 0.014		50 ± 19		0.34 ± 0.22
K47	2.65 ± 0.04	7.37 ± 0.14	0.67 ± 0.02	m2	0.787 ± 0.009		40 ± 11		
Y48	2.72 ± 0.03	7.51 ± 0.12	0.65 ± 0.02	m2	0.803 ± 0.008		55 ± 9		
K49	2.36 ± 0.03	5.84 ± 0.12	0.38 ± 0.02	m5	0.574 ± 0.025	0.782 ± 0.015		1083 ± 236	
P50									
N51	1.75 ± 0.03	3.62 ± 0.10	-0.25 ± 0.02	m5	0.283 ± 0.019	0.677 ± 0.010		962 ± 82	
M52	1.30 ± 0.02	2.14 ± 0.08	-2.18 ± 0.05	m2	0.123 ± 0.005			226 ± 7	
T53	0.79 ± 0.01	0.99 ± 0.07	-2.31 ± 0.01	m5	0.027 ± 0.011	0.466 ± 0.013		495 ± 56	

Supplementary Table 3. SpoVTN ¹⁵N relaxation and dynamics parameters (pH 5.8, 305.15 K, 399.8636182 MHz)

Residue	R_1 (s^{-1})	R_2 (s^{-1})	NOE	Model	S^2	S_f^2	$\tau_e < 100$ or τ_f (ps)	$\tau_e > 100$ or τ_s (ps)	R_{ex} (s^{-1})
<i>Monomer A</i>									
M1									
K2									
A3	1.88 ± 0.06	3.92 ± 0.14	-0.27 ± 0.03	<i>m5</i>	0.288 ± 0.027	0.739 ± 0.021		1015 ± 110	
T4	1.93 ± 0.07	4.46 ± 0.16	0.04 ± 0.04	<i>m5</i>	0.365 ± 0.031	0.707 ± 0.021		1125 ± 181	
G5	2.22 ± 0.07	5.37 ± 0.17	0.28 ± 0.04	<i>m5</i>	0.443 ± 0.033	0.768 ± 0.023		1501 ± 222	
I6	2.43 ± 0.09	7.36 ± 0.23	0.64 ± 0.05	<i>m2</i>	0.733 ± 0.019		45 ± 19		
V7	2.56 ± 0.09	7.70 ± 0.24	0.73 ± 0.06	<i>m1</i>	0.788 ± 0.019				
R8	2.69 ± 0.11	8.04 ± 0.30	0.67 ± 0.06	<i>m1</i>	0.827 ± 0.022				
R9	2.44 ± 0.08	7.48 ± 0.24	0.66 ± 0.05	<i>m2</i>	0.751 ± 0.020		38 ± 19		
I10	2.63 ± 0.09	8.64 ± 0.25	0.70 ± 0.05	<i>m1</i>	0.853 ± 0.020				
D11	2.59 ± 0.09	9.11 ± 0.25	0.70 ± 0.05	<i>m3</i>	0.827 ± 0.030				0.76 ± 0.38
D12	2.54 ± 0.08	7.12 ± 0.19	0.64 ± 0.04	<i>m5</i>	0.648 ± 0.044	0.803 ± 0.027		2752 ± 1446	
L13	2.62 ± 0.09	7.98 ± 0.23	0.67 ± 0.04	<i>m2</i>	0.802 ± 0.019		46 ± 24		
G14	2.63 ± 0.09	8.68 ± 0.28	0.69 ± 0.05	<i>m1</i>	0.853 ± 0.020				
R15									
V16	2.47 ± 0.11	9.09 ± 0.34	0.68 ± 0.07	<i>m3</i>	0.792 ± 0.034				1.00 ± 0.49
V17	2.45 ± 0.09	9.11 ± 0.28	0.66 ± 0.06	<i>m4</i>	0.786 ± 0.030		49 ± 28		0.77 ± 0.42
I18	2.45 ± 0.09	7.39 ± 0.23	0.53 ± 0.05	<i>m2</i>	0.732 ± 0.019		87 ± 21		
P19									
K20									
E21	2.60 ± 0.09	9.11 ± 0.28	0.76 ± 0.05	<i>m1</i>	0.863 ± 0.019				
I22	2.71 ± 0.11	8.33 ± 0.27	0.69 ± 0.06	<i>m1</i>	0.843 ± 0.021				
R23									
R24	2.53 ± 0.08	8.79 ± 0.22	0.70 ± 0.04	<i>m1</i>	0.836 ± 0.015				
T25	2.47 ± 0.08	8.30 ± 0.23	0.69 ± 0.04	<i>m2</i>	0.790 ± 0.018		38 ± 20		
L26									
R27	2.72 ± 0.09	8.62 ± 0.26	0.71 ± 0.06	<i>m1</i>	0.859 ± 0.019				
I28	2.55 ± 0.09	8.89 ± 0.29	0.68 ± 0.06	<i>m1</i>	0.843 ± 0.021				
R29	2.56 ± 0.10	7.91 ± 0.25	0.66 ± 0.05	<i>m2</i>	0.793 ± 0.020		47 ± 27		
E30	2.54 ± 0.07	7.26 ± 0.18	0.70 ± 0.03	<i>m5</i>	0.631 ± 0.047	0.787 ± 0.017		5182 ± 1828	
G31	2.58 ± 0.11	9.05 ± 0.34	0.76 ± 0.07	<i>m3</i>	0.810 ± 0.035				1.05 ± 0.47
D32	2.66 ± 0.08	8.84 ± 0.19	0.75 ± 0.04	<i>m1</i>	0.866 ± 0.014				
P33									
L34	2.54 ± 0.07	7.82 ± 0.17	0.62 ± 0.03	<i>m2</i>	0.781 ± 0.013		63 ± 15		
E35	2.67 ± 0.10	8.38 ± 0.29	0.65 ± 0.06	<i>m2</i>	0.831 ± 0.023		70 ± 43		
I36	2.73 ± 0.13	8.54 ± 0.38	0.70 ± 0.08	<i>m1</i>	0.860 ± 0.026				
F37	2.73 ± 0.13	9.04 ± 0.41	0.70 ± 0.09	<i>m1</i>	0.885 ± 0.029				
V38									
D39	2.60 ± 0.10	8.30 ± 0.28	0.65 ± 0.06	<i>m2</i>	0.818 ± 0.021		60 ± 39		

Supplementary Table 2 continued

Supplementary Table 3. SpoVTN ^{15}N relaxation and dynamics parameters (pH 5.8, 305.15 K, 399.8636182 MHz)

Residue	R_1 (s^{-1})	R_2 (s^{-1})	NOE	Model	S^2	S_f^2	$\tau_e < 100$ or τ_f (ps)	$\tau_e > 100$ or τ_s (ps)	R_{ex} (s^{-1})
R24	2.53 ± 0.08	8.79 ± 0.22	0.70 ± 0.04	m1	0.835 ± 0.016				
T25	2.47 ± 0.08	8.30 ± 0.23	0.69 ± 0.04	m2	0.790 ± 0.017		38 ± 20		
L26									
R27	2.72 ± 0.09	8.62 ± 0.26	0.71 ± 0.06	m1	0.858 ± 0.020				
I28	2.55 ± 0.09	8.89 ± 0.29	0.68 ± 0.06	m1	0.843 ± 0.019				
R29	2.56 ± 0.10	7.91 ± 0.25	0.66 ± 0.05	m2	0.792 ± 0.018		48 ± 28		
E30	2.54 ± 0.07	7.26 ± 0.18	0.70 ± 0.03	m5	0.638 ± 0.043	0.787 ± 0.018		5054 ± 1884	
G31	2.58 ± 0.11	9.05 ± 0.34	0.76 ± 0.07	m3	0.810 ± 0.033				1.04 ± 0.47
D32	2.66 ± 0.08	8.84 ± 0.19	0.75 ± 0.04	m1	0.865 ± 0.016				
P33									
L34	2.54 ± 0.07	7.82 ± 0.17	0.62 ± 0.03	m2	0.781 ± 0.013		63 ± 14		
E35	2.67 ± 0.10	8.38 ± 0.29	0.65 ± 0.06	m2	0.831 ± 0.022		70 ± 40		
I36	2.73 ± 0.13	8.54 ± 0.38	0.70 ± 0.08	m1	0.860 ± 0.028				
F37	2.73 ± 0.13	9.04 ± 0.41	0.70 ± 0.09	m1	0.885 ± 0.028				
V38									
D39	2.60 ± 0.10	8.30 ± 0.28	0.65 ± 0.06	m2	0.818 ± 0.022		60 ± 41		
R40	2.46 ± 0.12	7.01 ± 0.30	0.60 ± 0.06	m2	0.720 ± 0.022		56 ± 23		
D41	2.39 ± 0.08	7.17 ± 0.21	0.59 ± 0.04	m2	0.718 ± 0.015		58 ± 16		
G42	2.34 ± 0.08	7.14 ± 0.21	0.61 ± 0.05	m2	0.714 ± 0.016		47 ± 15		
E43	2.56 ± 0.08	7.54 ± 0.21	0.63 ± 0.04	m2	0.766 ± 0.017		60 ± 20		
V44	2.57 ± 0.10	8.54 ± 0.30	0.69 ± 0.06	m1	0.837 ± 0.022				
I45									
L46	2.62 ± 0.11	9.00 ± 0.32	0.73 ± 0.07	m3	0.824 ± 0.035				0.84 ± 0.45
K47	2.62 ± 0.11	8.29 ± 0.29	0.69 ± 0.07	m1	0.832 ± 0.022				
K48									
Y49	2.59 ± 0.10	7.94 ± 0.26	0.68 ± 0.06	m2	0.792 ± 0.020		44 ± 30		
S50	2.24 ± 0.07	6.11 ± 0.16	0.40 ± 0.03	m5	0.568 ± 0.029	0.763 ± 0.041		1097 ± 335	
P51									
I52	1.75 ± 0.04	3.10 ± 0.11	-0.39 ± 0.02	m5	0.178 ± 0.019	0.697 ± 0.016		1187 ± 62	
S53	1.57 ± 0.05	2.56 ± 0.11	-0.89 ± 0.03	m5	0.131 ± 0.021	0.694 ± 0.021		906 ± 65	
E54	1.30 ± 0.04	1.80 ± 0.10	-1.76 ± 0.05	m5	0.065 ± 0.017	0.681 ± 0.018		630 ± 56	
L55	0.90 ± 0.03	1.12 ± 0.09	-1.65 ± 0.02	m5	0.023 ± 0.015	0.458 ± 0.016		755 ± 55	

Table S4. Average DNA Base Pair and Base Pair step Parameters Prior and Post Docking

Parameters ^{a,b}	Prior – docking	Post – docking ^c
Twist (35.9° _{0.9})	36.0° _{0.7}	36.63° _{1.96}
Roll (-0.2° _{2.3})	1.7° _{0.2}	-0.06° _{3.85}
Tilt (0.0° _{0.1})	-0.01° _{0.48}	-0.13° _{2.74}
Rise (3.4 Å _{0.0})	3.4 Å _{0.0}	3.40 Å _{0.14}
Slide (0.3 Å _{0.2})	0.46 Å _{0.03}	0.56 Å _{0.51}
Shift (0.0 Å _{0.1})	0.00 Å _{0.02}	-0.08 Å _{0.44}
Opening (-3.3 Å _{2.5})	-1.68 Å _{0.28}	1.86 Å _{3.45}
Propeller (-10.2° _{7.3})	-10.2° _{7.3}	3.15° _{2.29}
Buckle (0.1° _{0.1})	0.05° _{0.56}	-0.23° _{2.62}
Stagger (0.1 Å _{0.0})	0.11 Å _{0.04}	-0.33 Å _{0.10}
Stretch (-0.1 Å _{0.0})	-0.12 Å _{0.04}	0.05 Å _{0.08}
Shear (0.0 Å _{0.1})	0.0 Å _{0.1}	0.04 Å _{0.26}
Minor groove width ^d	5.9 Å	6.5 Å
Major groove width ^d	11.4 Å	10.5 Å

^aThe average values for the canonical B-DNA input structure are shown in the left column between brackets next to each parameter.

^bStandard deviations are shown as subscripts.

^cValues from the lowest HADDOCK score structure.

^dAverage values.

Table S5. Active and Passive Residues of AbrBN⁵⁵-Tetramer and *abrB8*

	Active ^a	Passive ^b
AbrBN ⁵⁵	R8, K9, R15, V17, I20, E21, R23, R24, L26 T23, G24, A25, C26, A27, T33, G34, G35, A36, A37,	M1, G5, I6, V7, E12, L13, G27, A29, E30, K31, D32, Y48 T22, A28, T32, A38, G176, A182, A185, C191
<i>abrB8</i>	T177, T178, T179, C180, C181, A186, T187, T188, G189, T190	

^aActive residues are described as residues with at least 40% solvent accessibility and known to be involved with binding.

^bPassive residues are described as residues with at least 40% solvent accessibility and are adjacent to active residues, these residues are not directly involved in binding.

SUPPLEMENTAL METHODS

Cloning of SpovTN

DNA fragments coding the N-terminal domain SpovVT were obtained through PCR utilizing the Stratagene QuikChange Site-Directed Mutagenesis Kit (inserting a TAA stop codon at residue 56 from a construct containing the DNA sequence of full length SpovVT). DNA sequencing confirmed that the desired constructs were obtained. SpovVTN was obtained with the following oligonucleotide primers obtained from IDT-DNA:

SpoVTN Stop Forward:

5'- GCA TAC TCC TTT GCA AAG TCT **TAA** AGC TCA CTG ATC GGA GAG -3'

SpoVTN Stop Reverse:

5'- CTC TCC GAT CAG TGA GCT **TTA** AGA CTT TGC AAA GGA GTA TGC -3'

¹⁵N Backbone Relaxation Measurements and Model-free Analysis of Backbone Motions

Buffers used for ¹⁵N relaxation experiments were similar to those used for structure determination with one exception – TCEP (1 mM) was used instead of DTT in the AbhN NMR buffer. R_1 and R_2 measurements were collected with fully interleaved planes acquired at nine and eight relaxation delay values, respectively, with one exception. AbhN T_1 time point measurements were collected individually. Relaxation delays were as follows: AbhN [$T_1 = 10$ (x2), 50, 100, 160, 220 (x2), 300, 410, 560 (x2), 820 ms], [$T_2 = 4$ (x2), 18, 34, 54, 76 (x2), 104, 140 (x2), 192 ms]; AbrBN [$T_1 = 1.5$ (x2), 60, 120, 190, 280 (x2), 380, 520, 710 (x2), 1040 ms], [$T_2 = 4$ (x2), 16, 32, 54, 80 (x2), 112, 160 (x2), 240 ms]; and SpoVTN [$T_1 = 1.5$ (x2), 60, 120, 190, 280 (x2), 380, 520, 710 (x2), 1040 ms], [$T_2 = 4$ (x2), 16, 32, 54, 80 (x2), 112, 160 (x2), 240 ms]. Three replicate $\{^1\text{H}\}$ -¹⁵N NOE spectra were recorded with proton saturation using a 4 s period of saturation and interleaved with the reference spectrum, which was recorded with a 5 s recycle delay and no saturation. The instrument temperature was calibrated using 100% methanol before each set of experiments. Pulse sequences were written in-house from methods previously described (Farrow *et al.*, 1994; Skelton, 1993). Relaxation data were processed and analyzed using the NMRPipe/NMRDraw software suite using a Lorentz-to-Gauss window function (Delaglio *et al.*, 1995). Peak intensities were quantitated using the nlinLS module of the NMRPipe. R_1 and R_2 relaxation rates were obtained by fitting the peak intensities as a function of relaxation delay time to a single exponential decay function using the Levenberg-Marquardt nonlinear least-squares fitting program Curvefit v1.4 (A. G. Palmer III, Columbia University). Monte Carlo simulations were performed to estimate the uncertainty in the fitted parameters. Experimental errors associated with R_1 and R_2 relaxation rates were estimated from the baseline noise and the calculated uncertainty in peak intensities for duplicate data sets collected with the same relaxation delays. Steady-state $\{^1\text{H}\}$ -¹⁵N NOE values were calculated as the ratio between cross-peak intensities with (I_{ref}) and without (I_{sat}) ¹H saturation ($I_{\text{sat}}/I_{\text{ref}}$) averaged over three replicate experiments and errors were obtained by

$$\sigma_{\text{NOE}} = [((\sigma_{\text{sat}} * I_{\text{ref}})^2 + (\sigma_{\text{ref}} * I_{\text{sat}})^2)/(I_{\text{ref}})]^{1/2}$$

¹⁵N relaxation data for some residues were not obtained due to unobserved or overlapped resonances, as well as for all proline residues. For AbhN, these residues include M1, K2, V6, R15, P19, D27, K46, K49, P50 and H51. For AbrBN, these residues include M1, K2, D11, I18, P19 and P50. For SpoVTN, these residues include M1, K2, R15, P19, K20, R23, L26, P33, V38, I45, K48 and P51. The average 10% trimmed relaxation values are as follows: AbhN [$R_1 = 2.70(\pm 0.10) \text{ s}^{-1}$, $R_2 = 7.87(\pm 0.62) \text{ s}^{-1}$, $\text{NOE} = 0.65(\pm 0.07)$]; AbrBN [$R_1 = 2.65(\pm 0.10) \text{ s}^{-1}$, $R_2 = 7.57(\pm 0.56) \text{ s}^{-1}$, $\text{NOE} = 0.65(\pm 0.06)$]; and SpoVTN [$R_1 = 2.49(\pm 0.18) \text{ s}^{-1}$, $R_2 = 7.74(\pm 1.20) \text{ s}^{-1}$, $\text{NOE} = 0.60(\pm 0.20)$].

The program PDBINTERTIA (A. G. Palmer III, Columbia University) was used to obtain inertia tensors and structure files rotated so the moments of inertia are aligned with the Cartesian axes and translated so that the center of mass is located at the origin. Diffusion tensor estimates for spherical, axially-symmetric and anisotropic motional models were determined using the programs R2R1_TM and QUADRIC_DIFFUSION (A. G. Palmer III, Columbia University), the latter of which was used to produce structures rotated into the diffusion frame for model-free analysis. Residue-specific 10% or 15% trimmed R_2/R_1 ratios were used for the diffusion tensor estimate calculation, eliminating residues with very fast internal motions ($\tau_c \ll \tau_m$; i.e., residues with low R_2/R_1 ratios or NOE values < 0.6) or significant R_{ex} contribution to R_2 (i.e., residues with elevated R_2/R_1 ratios) (Jarymowycz and Stone, 2006). χ^2 and F statistics reported by QUADRIC_DIFFUSION were initially used to determine the appropriate diffusion tensor.

The initial global rotational correlation time (τ_c) estimates and D_{\parallel}/D_{\perp} values were set as follows: AbhN [isotropic: $\tau_c=6.54$ ns; axial prolate: $\tau_c=6.57$ ns; $D_{\parallel}/D_{\perp}=1.18$], AbrBN⁵³ [isotropic: $\tau_c=6.39$ ns; axial prolate: $\tau_c=6.35$ ns; $D_{\parallel}/D_{\perp}=1.11$], SpoVTN [isotropic: $\tau_c=6.91$ ns; axial prolate: $\tau_c=6.94$ ns; $D_{\parallel}/D_{\perp}=1.22$]. The τ_c values are consistent with the molecular size of a 10-12 kDa dimer in solution (Benson *et al.*, 2002; Bobay *et al.*, 2004; Bobay *et al.*, 2006; Dong *et al.*, 2004; Yao and Strauch, 2005). Values for the ¹⁵N CSA and N-H bond length (r_{NH}) were set to -172 ppm and 1.02Å, respectively, and Newton minimization was used for all calculations. The quality of the fits between the experimental data and each of the motional models and subsequent model selection was determined using previously described methods of model elimination (d'Auvergne and Gooley, 2006), χ^2 and Akaike's Information Criteria (AIC) statistics (d'Auvergne and Gooley, 2003) in the form of $AIC=\chi^2+2k$, where k is the number of model-free parameters in the model and χ^2 describes fit of the relaxation data to the model. A dimer symmetry-forced model selection protocol was used, where the number of datasets (n), k and χ^2 for symmetry equivalent residues were summed before AIC model selection, resulting in the selection of identical models for symmetric residues between the individual monomers of the dimer structure. Parameter fitting errors were determined using 500 Monte Carlo simulations.

The S^2 generalized order parameter is related to the equilibrium distribution of the N-H bond vector orientations; a value of 0 indicates completely unrestricted motion, whereas a value of 1 indicates completely restricted motion. The R_{ex} parameter describes the chemical exchange broadening contribution to the R_2 rate constant on the μ s-ms time scale. Other parameters and parametric restrictions resulting in the five mathematical motional models described above have been described previously (Clare *et al.*, 1990; Clare, 1990; Jarymowycz and Stone, 2006; Mandel *et al.*, 1995).

Several criteria were used to determine the diffusion tensor model and parameters most appropriate for fitting the relaxation data, including (1) F statistics describing the tensor estimations, as detailed above; (2) χ^2 and AIC statistics describing the fit of the relaxation data when assuming an isotropic or axial prolate tensor; and (3) the agreement between experimental and back-calculated ¹⁵N relaxation parameters.

HADDOCK Docking Procedure

The coordinate file for AbrBN⁵⁵-tetramer was obtained by modeling the first 55 residues of AbrB against the solved structure of AbrBN by MODELLER (7v2) (Sali *et al.*, 1995). The resulting models were analyzed by their respective outputs from PROCHECK and their energy function output from MODELLER (Laskowski *et al.*, 1996; Sali *et al.*, 1995). The *abrB8* sequence 5'-ATG ATT GAC AAT TAT TGG AAA CCT -3' was used in this study (Xu *et al.*, 1996). A model of canonical C2'-endo conformation B-DNA was generated by 'DNA Tools'

(<http://hydra.icgeb.trieste.it/~kristian/dna/>) through a trinucleotide base pair parameter with AMBER minimization.

N-terminal domain mutations that disrupt AbrB binding to DNA are: R8S, K9R, G14A, R15H/S, V17A, I18G, P19A, I20L/S, E21A, L22R, R23S, R24S, L26R, I28G/R, L34H and C54S/Y/W (unpublished results). Of these R8, K9, R15, V17, I20, E21, L22, R23, R24 and L26 are defined as active. Residues G14, I18, P19, I28 and L34 are not solvent accessible. Residues M1, G5-V7, E12-L13, G27, A29, E30-D32 and Y48 are defined as passive. The promoter region of *abrB8* contains an asymmetric TGNNA-5bp-TGGNA binding motif, which has been shown to be a very loosely conserved sequence recognized by AbrB (Xu and Strauch, 1996). These base pairs (base pairs T6-A10, T16-T20, T4'-G8', and T14'-T18') were defined as the active region while two base pairs on either side of the TGNNA-5bp-TGGNA motif were defined as passive (base pairs T5, A11, T15, A21, C3', G9', A13', and T19') (Xu *et al.*, 1996).

Watson–Crick base pairs were defined and hydrogen bond lengths of the input structure were measured and restricted to $\pm 0.05 \text{ \AA}$. Sugar-phosphate backbone dihedral angles of the input structure were measured and used as restraints (restricted to $\alpha = \alpha_{\text{inp}} \pm 10^\circ$, $\beta = \beta_{\text{inp}} \pm 40^\circ$, $\gamma = \gamma_{\text{inp}} \pm 20^\circ$, $\delta = \delta_{\text{inp}} \pm 50^\circ$, $\epsilon = \epsilon_{\text{inp}} \pm 10^\circ$ and $\zeta = \zeta_{\text{inp}} \pm 50^\circ$), similar to other published protein:DNA interactions determined using HADDOCK (van Dijk *et al.*, 2006).

Planarity restraints for the purine and pyrimidine rings were introduced and the sugar pucker was restrained to the C2'-endo conformation to preserve DNA helical conformation. Consecutive phosphorus to phosphorus distances were measured and restricted to 6.0–7.5 Å. In order to preserve symmetry of the AbrBN⁵⁵-tetramer, a non-crystallographic symmetry energy term (NCS) and distance symmetry potential were used to keep the C α atoms of the monomers superimposable. The H-bonding network of unbound AbrBN was employed as a restraint to maintain similar dimerization interfaces between the unbound and bound structures. Disulfide restraints in the AbrBN⁵⁵-tetramer were restricted to 2.0 \pm 0.25 nm. Systematic sampling of 180° rotated solutions was used in the rigid-body docking stage to minimize the occurrence of false positives.

SUPPLEMENTAL REFERENCES

Benson, L.M., Vaughn, J.L., Strauch, M.A., Bobay, B.G., Thompson, R., Naylor, S., and Cavanagh, J. (2002). Macromolecular assembly of the transition state regulator AbrB in its unbound and complexed states probed by microelectrospray ionization mass spectrometry. *Anal Biochem* 306, 222-227.

Bobay, B.G., Benson, L., Naylor, S., Feeney, B., Clark, A.C., Goshe, M.B., Strauch, M.A., Thompson, R., and Cavanagh, J. (2004). Evaluation of the DNA binding tendencies of the transition state regulator AbrB. *Biochemistry* 43, 16106-16118.

Bobay, B.G., Mueller, G.A., Thompson, R.J., Murzin, A.G., Venters, R.A., Strauch, M.A., and Cavanagh, J. (2006). NMR structure of AbhN and comparison with AbrBN: FIRST insights into the DNA binding promiscuity and specificity of AbrB-like transition state regulator proteins. *J Biol Chem* 281, 21399-21409.

Clore, G. M., Driscoll, P. C., Wingfield, P. T., and Gronenborn, A. M. (1990). Analysis of the backbone dynamics of interleukin-1 beta using two-dimensional inverse detected heteronuclear 15N-1H NMR spectroscopy. *Biochemistry* 29, 7387-7401.

Clore, G. M., Szabo, A., Bax, A., Kay, L.E., Driscoll, P.C., and Gronenborn, A.M. (1990). Deviations from the Simple 2-Parameter Model-Free Approach to the Interpretation of N-15 Nuclear Magnetic-Relaxation of Proteins. *Journal of the American Chemical Society* 112, 4989-4991.

d'Auvergne, E. J., and Gooley, P. R. (2003). The use of model selection in the model-free analysis of protein dynamics. *J Biomol NMR* 25, 25-39.

d'Auvergne, E. J., and Gooley, P. R. (2006). Model-free model elimination: a new step in the model-free dynamic analysis of NMR relaxation data. *J Biomol NMR* 35, 117-135.

Delaglio, F., Grzesiek, S., Vuister, G. W., Zhu, G., Pfeifer, J., and Bax, A. (1995). NMRPipe: a multidimensional spectral processing system based on UNIX pipes. *J Biomol NMR* 6, 277-293.

Dong, T.C., Cutting, S.M., and Lewis, R.J. (2004). DNA-binding studies on the *Bacillus subtilis* transcriptional regulator and AbrB homologue, SpoVT. *FEMS Microbiol Lett* 233, 247-256.

Farrow, N. A., Muhandiram, R., Singer, A. U., Pascal, S. M., Kay, C. M., Gish, G., Shoelson, S. E., Pawson, T., Forman-Kay, J. D., and Kay, L. E. (1994). Backbone dynamics of a free and phosphopeptide-complexed Src homology 2 domain studied by ¹⁵N NMR relaxation. *Biochemistry* 33, 5984-6003.

Jarymowycz, V. A., and Stone, M. J. (2006). Fast time scale dynamics of protein backbones: NMR relaxation methods, applications, and functional consequences. *Chem Rev* 106, 1624-1671.

Laskowski, R. A., Rullmann, J. A., MacArthur, M. W., Kaptein, R., and Thornton, J. M. (1996). AQUA and PROCHECK-NMR: programs for checking the quality of protein structures solved by NMR. *J Biomol NMR* 8, 477-486.

Mandel, A. M., Akke, M., and Palmer, A. G., 3rd (1995). Backbone dynamics of *Escherichia coli* ribonuclease HI: correlations with structure and function in an active enzyme. *J Mol Biol* 246, 144-163.

Sali, A., Potterton, L., Yuan, F., van Vlijmen, H., and Karplus, M. (1995). Evaluation of comparative protein modeling by MODELLER. *Proteins* 23, 318-326.

Skelton, N. J., Palmer III, A.G., Akke, M., Kordel, J., Rance, M., and Chazin, W.J. (1993). Practical Aspects of Two-Dimensional Proton-Detected ¹⁵N spin Relaxation Measurements. *Journal of Magnetic Resonance* 102, 253-264.

van Dijk, M., van Dijk, A. D., Hsu, V., Boelens, R., and Bonvin, A. M. (2006). Information-driven protein-DNA docking using HADDOCK: it is a matter of flexibility. *Nucleic Acids Res* 34, 3317-3325.

Yao, F., and Strauch, M.A. (2005). Independent and interchangeable multimerization domains of the AbrB, Abh, and SpoVT global regulatory proteins. *J Bacteriol* 187, 6354-6362.

Xu, K., and Strauch, M. A. (1996). In vitro selection of optimal AbrB-binding sites: comparison to known in vivo sites indicates flexibility in AbrB binding and recognition of three-dimensional DNA structures. *Mol Microbiol* 19, 145-158.

Xu, K., Clark, D., and Strauch, M. A. (1996). Analysis of abrB mutations, mutant proteins, and why abrB does not utilize a perfect consensus in the -35 region of its sigma A promoter. *J Biol Chem* 271, 2621-2626.